ORIGINAL ARTICLE

Intrinsic Fibrillation of Fast-Acting Insulin Analogs

R. Jeremy Woods, Ph.D., Javier Alarcón, M.S., Elaine McVey, M.S., and Ronald J. Pettis, Ph.D.

Abstract

Background:

Aggregation of insulin into insoluble fibrils (fibrillation) may lead to complications for diabetes patients such as reduced insulin potency, occlusion of insulin delivery devices, or potentially increased immunological potential. Even after extensive investigation of fibril formation in regular human insulin, there are little published data about the intrinsic fibrillation of fast-acting analogs. This article investigates and compares the intrinsic fibrillation of three fast-acting insulin analogs—lispro, aspart, and glulisine—as a function of their primary protein structure and exclusive of the stabilizing excipients that are added to their respective commercial formulations.

Methods:

The insulin analogs underwent a buffer exchange into phosphate-buffered saline to remove formulation excipients and then were heated and agitated to characterize intrinsic fibrillation potentials devoid of excipient stabilizing effects. Different analytical methods were used to determine the amount of intrinsic fibrillation for the analogs. After initial lag times, intrinsic fibrillation was detected by an amyloid-specific stain. Precipitation of insulin was confirmed by ultraviolet analysis of soluble insulin and gravimetric measurement of insoluble insulin. Electron microscopy showed dense fibrous material, with individual fibrils that are shorter than typical insulin fibrils. Higher resolution kinetic analyses were carried out in 96-well plates to provide more accurate measures of lag times and fibril growth rates.

Results:

All three analogs exhibited longer lag times and slower intrinsic fibrillation rates than human insulin, with glulisine and lispro rates slower than aspart. This is the first study comparing the intrinsic fibrillation of fast-acting insulin analogs without the stabilizing excipients found in their commercial formulations.

Conclusions:

Data show different intrinsic fibrillation potentials based on primary molecular structures when the formulation excipients that are critical for stability are absent. Understanding intrinsic fibrillation potential is critical for evaluating insulin analog stability and device compatibility.

J Diabetes Sci Technol 2012;6(2):265-276

Introduction

Protein aggregation is a constant risk during the manufacture, storage, and administration of biopharmaceuticals.[1–6] Users of biopharmaceuticals are potentially vulnerable to the harmful effects of aggregation, such as reduced drug bioactivity and possible immunogenic responses to the resulting protein particles.[4,7,8] Different molecular mechanisms can cause protein aggregation. One mechanism is protein denaturation with subsequent misfolding or aggregation, resulting in amyloid fibril formation.[1,5,6] Although some proteins are more susceptible than others, it is believed that most proteins can form amyloid fibrils under appropriate denaturing conditions.[9] Intrinsic fibrillation of endogenous proteins and peptides is a common theme for a variety of neurodegenerative diseases such as Alzheimer's, Parkinson's, and Huntington's.[10,11] The mechanism of protein fibrillation is rooted in partial protein or peptide denaturation or misfolding, leading to fibril nucleus formation.[12] This nucleus catalyzes a rapid and irreversible cascade of amyloid fibril growth. The structural hallmark of all amyloid fibrils is a stacked parallel β-sheet structure.[13–15]

The fibril-forming nature of regular human insulin is well characterized, and it is often used as a model protein for studying intrinsic protein fibrillation.[16–25] Formation of insulin fibrils within pharmaceutical preparations reduces the bioactivity of the drug and may be one of the causes of occlusion in continuous insulin infusion sets.[26] Either of these situations can result in diabetic ketoacidosis, a life-threatening complication.[27] The key to avoiding insulin intrinsic fibrillation is maintenance of the hexameric state prior to injection, because the monomer is more prone to hydrophobic surface-induced denaturation and intrinsic fibrillation.[21] Commercial insulin preparations are formulated with excipients to promote this high-order conformation and help maintain stability. In the presence of zinc, regular human insulin exists as a hexamer that is composed of three dimers. The phenolic excipients that are added to insulin preparations also promote a particularly stable hexameric conformation known as R-hexamer.[28–30]

Despite the attention paid to fibrillation in regular human insulin preparations, there are little published data available about the intrinsic fibrillation potential of the newer fast-acting insulin analogs in common use today. These analogs have strategic amino acid substitutions in the B chain (listed in **Table 1**) designed to limit

self-association into hexamers.[31–33] These substitutions result in greater monomeric nature, leading to faster dissociation, absorption, and biological action after injection.[34–38] The resulting changes in self-association may also have implications for the intrinsic fibrillation of the various analogs.

The common feature of lispro and aspart is substitution of the B28 proline, which is critical in the formation of the monomer–monomer β-sheet interfaces involved in insulin dimerization.[37] These amino acid substitutions prevent dimerization, increasing the monomeric nature of the analogs. However, lispro and aspart do form zinc–insulin hexamers in the presence of the phenolic excipients present in commercial pharmaceutical formulations.[29,31] Allosteric interactions of the analogs with these phenolic excipients lead to hexamers resembling the human insulin R-hexamer. After injection, diffusion of these phenolic excipients, zinc dissociation, and insulin dilution contribute to rapid hexamer dissociation into active and readily absorbed monomers.

The glulisine analog is incapable of forming zinc–insulin hexamers because of steric and electrostatic effects from the B3 lysine substitution.[37] Also, the B29 glutamic acid substitution reduces but does not prevent dimerization. Glulisine contains an intramolecular salt bridge between the N terminus of the A chain and the B29 glutamic acid, increasing monomer stability. Polysorbate 20, found in glulisine preparations, also acts as a surfactant that further limits surface-induced monomer denaturation at the hydrophobic air–water interface.[39]

Insulin analog formulations currently in use have been designed and extensively tested to maintain stability in

Table 1. Amino Acid Substitutions in Fast-Acting Insulin Analogs[a]			
	Amino acid position		
Insulin analog	B3	B28	B29
Human	Asparagine	Proline	Lysine
Lispro	Asparagine	*Lysine*	*Proline*
Aspart	Asparagine	*Aspartic acid*	Lysine
Glulisine	*Lysine*	Proline	*Glutamic acid*
[a] Amino acid substitutions appear in italics.			

their original primary containers when stored and used appropriately under the manufactures' recommended storage and shelf-life conditions. However, improper storage, handling, or interactions with medical devices introduce the potential for deleterious changes in both the insulin formulations and the insulin protein. This article evaluates several methods to assess the intrinsic fibrillation of fast-acting insulin analogs and subsequently compares their intrinsic fibrillation rates in the presence of heat and agitation and without the stabilizing excipients that are added to the respective commercial formulations. Intrinsic fibrillation of the analogs was demonstrated by the binding of the fibril-specific dye thioflavine T (ThT), increasing turbidity, and electron microscopy. Complete insulin precipitation was confirmed by ultraviolet (UV) absorbance quantification of soluble insulin and gravimetric quantification of insoluble insulin. Subsequent analysis using an automated 96-well plate format with higher sampling frequency was used to provide a more accurate quantification of intrinsic fibrillation kinetics. This kinetic analysis showed the same relative order of insulin analog intrinsic fibrillation rates, but all were more stable than regular human insulin.

This article represents an early investigation of methods useful for examining the aggregation potential of insulin analogs and an initial comparison of preliminary intrinsic fibrillation rates between the common analogs under conditions designed to exacerbate aggregation.

Materials and Methods

Materials

Insulin lispro (Humalog[TM], Lilly, Indianapolis, IN), insulin glulisine (Apidra[TM], Sanofi-Aventis, Bridgewater, NJ), insulin aspart (NovoLog[TM], Novo Nordisk, Bagsværd, Denmark), and recombinant human insulin (Humulin R[TM], Lilly, Indianapolis, IN) were purchased in their commercial formulations from a retail pharmacy. All insulin solutions had greater than 1 year of shelf life remaining at time of use, and were stored at the manufacturers' recommended storage conditions. Other materials and supplies were obtained from commercial sources and used as provided.

Insulin Sample Preparation

The commercial formulation buffers of the insulin analogs were exchanged for phosphate-buffered saline (PBS) using desalting spin columns to remove formulation excipients. Desalting spin columns (Zeba 7K MWCO, Pierce, Rockford, IL) were pre-equilibrated by washing

with three column volumes of PBS (pH 7.5 ± 0.01; Mediatech, Manassas, VA). The PBS wash was discarded, and the insulin analog was loaded onto the columns (2.2 ml insulin per column) followed by a spin elution for 3 min at 1500 G. Eluted insulin was collected and pooled to prepare approximately 90 ml per insulin analog. The pooled insulin concentration was determined using the extinction coefficient of 0.9521 ml/mg^{-1}/cm^{-1} at 277.5 nm absorbance.[40] The final concentration of each insulin analog was subsequently adjusted to 3.0 mg/ml with PBS buffer for most studies except as indicated. Buffer exchange on fresh analog samples was performed immediately prior to initiation of all fibrillation studies, and no buffer-exchanged samples were stored for later use. Examination of post-column eluates of the analog formulations was performed on representative samples using various analytical techniques to confirm the removal of added excipients (data not shown). Quadrupole mass spectrometry confirmed removal of the surfactant and tonicity agents, Tween 20 and glycerol. Similarly, removal of the phenolic preservatives/conformation stabilizers, m-cresol and phenol, was confirmed by reversed-phase high-performance liquid chromatography (HPLC). Soluble zinc levels were reduced by approximately 10%, as monitored by inductively coupled plasma-mass spectrometry.

Circular Dichroism

Near-UV circular dichroism (CD) spectra (250–300 nm) were obtained for analogs in PBS buffer-exchanged samples and in original formulations on a Jasco J810-150S spectrapolarimeter (Easton, MD) at 22 °C. Spectra were also obtained for PBS alone and insulin-free buffers containing all formulation excipients for each insulin analog, prepared at levels specified in manufacturer package inserts. These negative control buffer spectra were subtracted from the respective insulin CD spectra. Samples were scanned in 1 mm path length quartz cuvettes at standard sensitivity, 2 nm bandwidth, 2 s response, 0.5 nm data pitch, and 20 nm/min scanning speed. A total of three scans was averaged for each sample.

Intrinsic Fibrillation of Insulin Analogs with Intermittent Sampling

Three replicates (15 ml each) per insulin analog (3.0 mg/ml in PBS) were prepared in 50 ml polypropylene conical tubes (BD Falcon, Franklin Lakes, NJ). The capped tubes were placed upright in a rack on a reciprocating shaker (Brinkmann, Germany) at 170 rpm within an incubator at 37 or 45 °C for up to 2 weeks. Aliquots (1.2 ml each) were removed by pipette at each time point, and these aliquots were divided for subsequent analyses.

Thioflavine T Assay

A saturated ThT solution was prepared by adding approximately 4 mg ThT dye (EMD, Gibbstown, NJ) to 1 ml PBS in a 1.5 ml microcentrifuge tube and vigorously vortexing for 1 min. The resulting solution was centrifuged at 16,000 G for 2 min to remove undissolved dye, and the supernatant was transferred to a new tube. The ThT concentration was determined by ultraviolet–visible (UV–Vis) spectroscopy using the extinction coefficient of 35 M^{-1} cm^{-1} at 412 nm and adjusted to a final 0.4 mM concentration by dilution with PBS (approximately 1:10 dilution).

Insulin analog samples (20 µl) were diluted with 75 µl PBS in a 96-well polystyrene plate (BD Falcon P/N 35-3948). Negative controls consisted of 95 µl PBS. Thioflavine T (0.4 mM, 5 µl) was added to the samples and controls for a final ThT concentration of 0.02 mM. The plate was mixed for 1 min on a titer plate shaker (Lab-line, P/N 01020164) at a 50% speed setting. The plate was then scanned on a fluorescence reader (BMG NOVOstar; top read; 450 nm excitation filter with 10 nm bandwidth; 520 nm emission filter with 35 nm bandwidth; gain 1000; 10 flashes; 10 s shaking at 350 rpm prior to scan). The fluorescence intensity of the PBS negative control was subtracted from the fluorescence values for the samples, and the resulting values were normalized by dividing by 15,000 to provide relative fluorescence values between 0 and 1 for graphing purposes. Fluorescence intensity is reported in arbitrary relative fluorescence units (RFUs).

Ultraviolet Measurement of Soluble Insulin and Gravimetric Measurement of Insoluble Aggregates

The insoluble material formed upon protein intrinsic fibrillation was collected and measured gravimetrically, with the remaining soluble insulin in the supernatant measured by UV spectroscopy, to determine the extent of aggregation and precipitation within the incubated insulin solutions. Samples (900 µl) were transferred to preweighed 1.5 ml microcentrifuge tubes and centrifuged at 16,000 G for 7 min. The absorbance of each supernatant solution at 277.5 nm was measured using a 1 cm path length quartz cuvette and a UV–Vis spectrophotometer, with soluble insulin concentrations determined by Beers Law using an extinction coefficient of 0.9521 $ml/mg^{-1}/cm^{-1}$.[40] Precipitate pellets were resuspended and washed with 1 ml water and recentrifuged, and the water wash was discarded. The washed pellets were frozen, dried under vacuum, and weighed to determine the mass of insoluble aggregates. This mass was divided by the original aliquot volume (900 µl) to obtain the concentration of insoluble insulin particles.

Transmission Electron Microscopy

At the final time points, aliquots (100 µl) of the incubated insulin solutions were collected and sent to the Chapel Hill Analytical and Nanofabrication Laboratory for transmission electron microscopy (TEM) according to published procedure.[21] Samples (5 µl) were dried on Formvar-coated carbon grids (Ted Pella, Inc.), rinsed five times with nanopure water, and negative stained five times with 1% uranyl acetate. Fibrils were imaged with a JEOL 100CX II microscope (JEOL USA, Inc) at 80 kV accelerating voltage.

Ninety-Six-Well Plate Intrinsic Fibrillation Kinetic Assay Using Turbidity Measurements for Regular Human Insulin and Insulin Analogs

The 96-well plate turbidity method allows for greater precision among replicates and a more accurate observation of lag time and intrinsic fibrillation rates due to more frequent sampling. The optical density at 600 nm was used as a quantitative indicator of the turbidity resulting from insoluble protein particles. Insulin analogs in PBS buffer were prepared as described earlier to a final concentration of 2.85 mg/ml. Five replicates of each analog (200 µl) were added to a 96-well polypropylene plate (Agilent Technologies, Santa Clara, CA). The plate was sealed with ultraclear, heat-resistant adhesive film for polymerase chain reaction plates (VWR, Suwanee, GA) and loaded into a UV–Vis plate reader (SpectraMax 190, Molecular Devices). The plate reader was set to kinetic analysis under the following settings: constant shaking, 45 °C, and 600 nm absorbance measurements every 400 s for 50 h.

Lag times and the intrinsic fibrillation growth rates for each analog were determined from the absorbance versus time data. The mean signal for all observations over the first hour was subtracted from each insulin analog replicate for baseline correction purposes. A linear region of the signal growth phase was selected for each analog (signal between 0.075 and 0.225 OD). Data from this region were fit using simple linear regression to obtain a value for the growth rate. The resulting coefficients were used to calculate the x intercept, which is the lag time. One replicate for insulin glulisine was discarded as an outlier due to substantially shorter lag time. The average lag times and growth rates for the replicates of analogs are reported here.

Results and Discussion

Preparation of Insulin Analogs

Each insulin analog is sold in a unique formulation buffer containing excipients for various purposes, including maintaining pH and isotonicity, acting as bacteriostatic preservatives, and promoting insulin conformational and chemical stability (**Table 2**). Some excipients such as the phenolic alcohols, m-cresol and phenol, may serve dual purposes as both preservatives for multidose containers and as stabilizing agents depending on the specific analog. The conformational stabilizing mechanism of the excipients depends on the particular analog. For example, zinc and phenolic excipients promote the stable hexameric state of lispro and aspart.[29,31] Glulisine, which does not form hexamers, utilizes a surfactant to protect the monomer from surface-induced denaturation.[37] Other unique buffer properties such as ionic strength and pH may also contribute to the stability of each analog. The conformational stabilizing effects of the formulation excipients are designed to maintain protein stability and thereby delay intrinsic fibrillation making comparisons between the intrinsic fibrillation potential among the insulin analogs difficult to examine.

To eliminate these effects of excipient stabilization and compare the intrinsic fibrillation rate of analog monomers and dimers, gel filtration was used to exchange formulation buffers for PBS, ensuring that all analogs were studied under essentially equivalent buffer conditions. Buffer exchange removed phenolic excipients that promote a more stable hexameric state in lispro and aspart[29,31] and also the various surfactants and tonicity agents as noted earlier.

Circular Dichroism

Near-UV CD was used to verify dissociation of lispro and aspart hexamers after transfer to PBS. This technique has been used previously to probe phenolic excipient effects on the hexameric state of various insulin types. The weak 251 nm ellipticity of human zinc–insulin hexamers is substantially enhanced when phenolic excipients are added, due to the transition from the native T hexamer to the more compact R-hexamer.[41] A similar ellipticity enhancement, corresponding to direct transition from monomer to the R-hexamer, occurs when zinc and phenolic excipients are added to insulin lispro monomers.[31]

Circular dichroism spectra from 250–260 nm, taken before and after buffer exchange, are shown in **Figure 1**.

Table 2.
Buffer Components and Excipients of Marketed Fast-Acting Insulin Formulations

	Lispro	Aspart	Glulisine
Buffer	Sodium phosphate	Sodium phosphate	Tromethamine
Metal	Zinc	Zinc	
Phenolic	M-cresol	M-cresol, phenol	M-Cresol
Surfactant			Polysorbate 20
Tonicity agents	Glycerol	Glycerol, sodium chloride	Sodium chloride
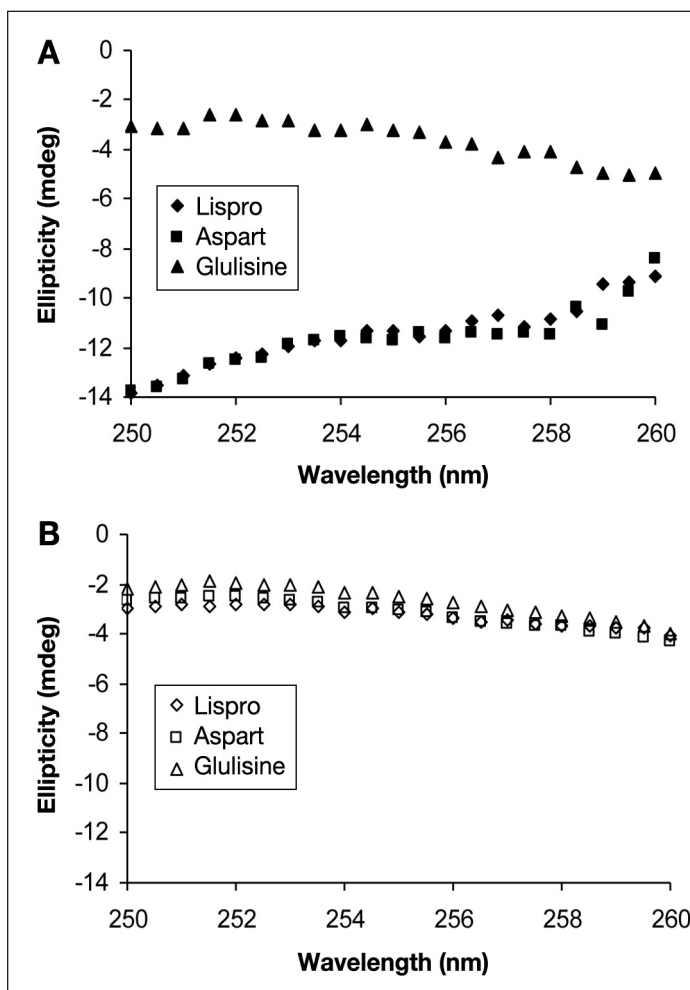
Figure 1. Near-UV CD of fast-acting insulin analogs (3.5 mg/ml) **(A)** in marketed formulations and **(B)** after transfer to PBS using gel filtration columns. Spectra were corrected for buffer excipients alone and are the average of three scans. Standard deviations are not shown for clarity but were ≤ 1.0 mdeg for each point in **(A)** and ≤ 0.2 mdeg for each point in **(B)**.

The ellipticity of lispro and aspart in this region is substantially stronger in the formulated solutions than in PBS, which is consistent with the formation of R-hexamers

in the presence of zinc and phenolic excipients.[29,31] The ellipticity of glulisine, which is not able to form hexamers,[37] is not enhanced in the pharmaceutical buffer. After transfer to PBS, the ellipticities of lispro and aspart decrease to the level of glulisine, confirming hexamer dissociation and the monomer/dimer conformations of all analogs.

While CD spectroscopy is effective for examining higher-order insulin association, alternative analytical techniques exist for separating and quantifying protein self-association, including ultracentrifugation, dynamic light scattering, and size exclusion high-performance liquid chromatography (SE-HPLC). In ongoing related efforts examining insulin analog self-association kinetics, SE HPLC using multiangle light scattering detection was used to confirm an initial primarily dimeric association state in all three analogs after equivalent buffer exchange and excipient removal.[42]

### Agitation of Insulin Solutions with Intermittent Sampling

Triplicate PBS solutions of each analog were agitated at 37 or 45 °C in polypropylene tubes to promote intrinsic fibrillation. Aliquots were removed at intermittent time points and assayed for ThT fluorescence, the concentration of soluble and insoluble insulin, and the turbidity. Heating and agitation are known to speed insulin intrinsic fibrillation and were incorporated to reduce intrinsic fibrillation times to a manageable timescale during these comparison studies. Hydrophobic surfaces such as plastics may promote intrinsic fibrillation by inducing partial denaturation of insulin monomers, and agitation compounds this effect by increasing the effective surface-area-to-water ratio.[16–19] Agitation may also speed the collisions between monomers and growing fibrils responsible for fibril growth.[43]

Thioflavine T Assay

Intrinsic fibrillation at both temperatures was monitored by measuring ThT fluorescence. Thioflavine T is a specific dye for amyloid fibrils that undergoes a fluorescence shift and a large increase in quantum yield upon fibril binding.[44,45] **Figure 2** shows dramatic increases in ThT RFUs after agitation of insulin analogs at both temperatures. A discernable lag time to initiation was noted in most of the replicates, with a ThT fluorescence plateau occurring shortly after initiation. Differences in the plateau intensities are apparent in **Figure 2**. These differences may be related to fibril polymorphism among the different analogs and conditions. Fibril morphology is highly dependent on amino acid sequence and on

external conditions,[43,46–48] and the morphology influences the fluorescence quantum yield of bound ThT.[48]

Plots in **Figure 2** show the lag time variability between the replicates for each insulin analog, with substantially higher variability at 37 °C than at 45 °C. This variability may reflect stochastic nucleation processes,[49,50] caused by minor uncontrolled differences in experimental
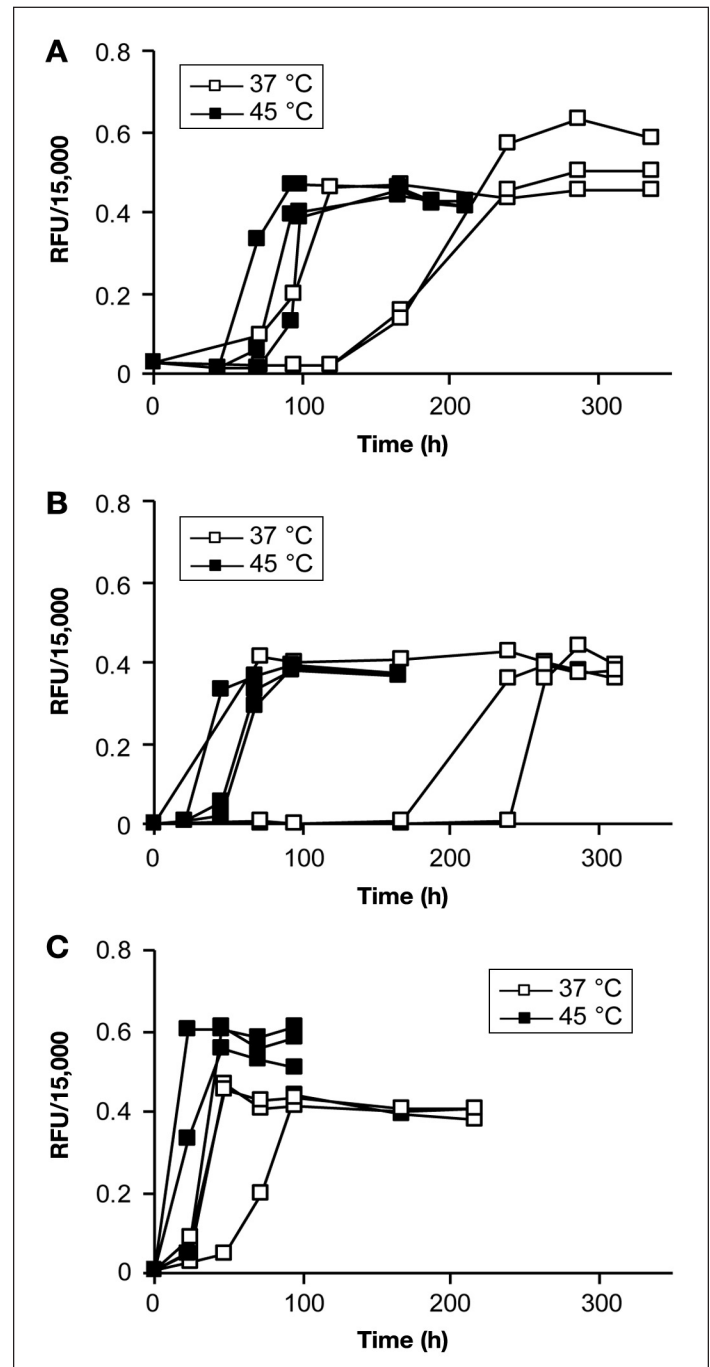
Figure 2. Intrinsic fibrillation of fast-acting insulin analogs in PBS monitored by ThT fluorescence with constant shaking at 37 or 45 °C: **(A)** lispro, **(B)** glulisine, and **(C)** aspart.

conditions, such as mixing and heating inhomogeneities, imperfections in the plastic tubes, or the presence of dust particles or air bubbles. Any of these factors can affect particle nucleation and contribute to variability.

Despite the noted variability among replicates, trends emerge from the fluorescence plots (**Figure 2**) and the calculated 50% intrinsic fibrillation rates (t_{50}; **Table 3**). Lag times are generally shorter at 45 °C than at 37 °C, reflecting the temperature influence on protein intrinsic fibrillation kinetics.[51,52] Higher temperatures may increase the partially denatured monomer population while simultaneously increasing the molecular collision rate, leading to intrinsic fibrillation. Faster kinetics at higher temperatures may mask the lag time variability seen at 37 °C. Differences among analogs are also apparent. Aspart lag times are shorter than those of lispro and glulisine at a given temperature. These differences are not surprising, given the highly sequence-dependent nature of protein and peptide intrinsic fibrillation kinetics.[53–55]

Precipitation of Insoluble Insulin

In all cases, ThT fluorescence increases are accompanied by increased turbidity that is visible to the naked eye, indicating the formation of insoluble material. Turbidity was quantitatively examined at 37 °C by measuring the absorbance at 600 nm. Insulin precipitation was also confirmed by measuring decreases in soluble insulin levels by UV absorbance at 277.5 nm and by gravimetric increases of collected insoluble insulin. These results are shown in **Figure 3** for a single replicate of each analog at 37 °C. Calculated t_{50} lag times shown in **Table 3** are nearly identical for each of these four methods. The concurrent changes in these markers are consistent with protein intrinsic fibrillation and precipitation of soluble protein into insoluble fibrils.
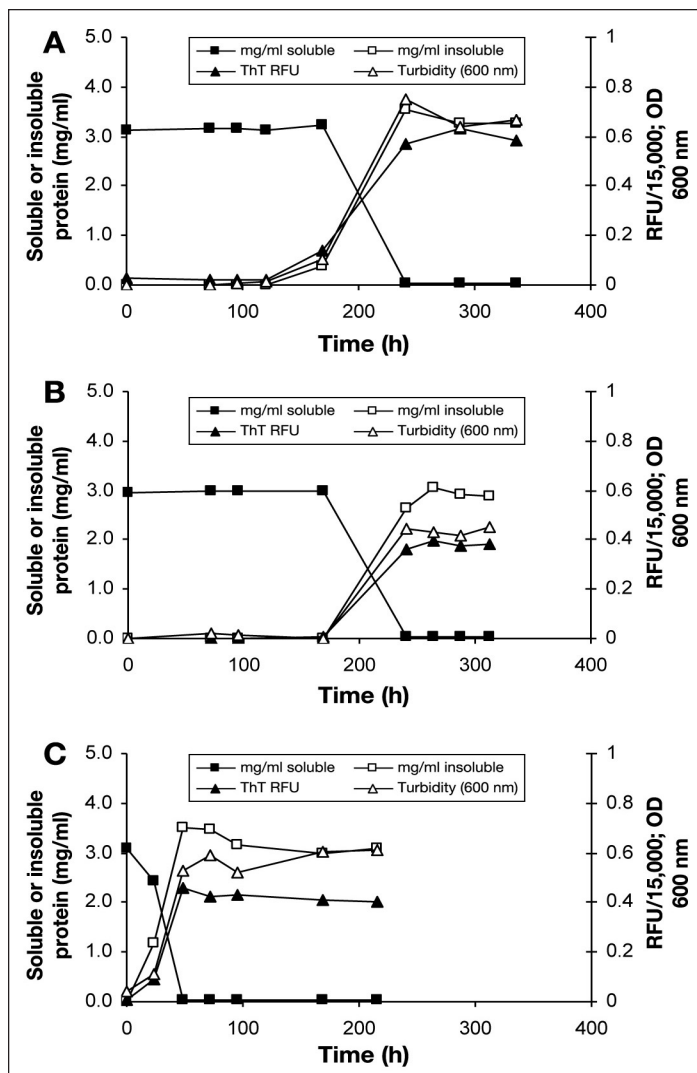

Figure 3. Intrinsic fibrillation of fast-acting insulin analogs in PBS at 37 °C, measured by ThT fluorescence, UV absorbance of soluble protein, gravimetric determination of insoluble insulin mass, and turbidity at 600 nm for **(A)** insulin lispro, **(B)** insulin glulisine, and **(C)** insulin aspart. A single representative replicate from $n = 3$ is shown for each analog. OD, optical density.

Table 3.

Average Time to 50% Insulin Intrinsic Fibrillation (t_{50}, hours), Measured by Four Different Analytical Methods[a]: ThT Fluorescence Increase, Loss of Soluble Insulin Concentration by Ultraviolet Absorbance at 412nm, Gravimetric Increase of Insoluble Insulin, and Turbidity Measured by Ultraviolet Absorbance at 600 nm

Method	Lispro		Glulisine		Aspart	
	37 °C	45 °C	37 °C	45 °C	37 °C	45 °C
ThT	164 (55)	79 (16)	166 (114)	50.7 (13)	47.5 (23)	20.9 (11)
Soluble insulin	166 (59)	77 (17)	166 (115)	49.1 (11)	47.6 (23)	20.7 (11)
Insoluble insulin	164 (58)	77 (18)	166 (114)	51.2 (13)	46.1 (22)	19.7 (11)
Turbidity (600 nm)[b]	164 (54)	N/A	166 (116)	N/A	48.9 (21)	N/A

[a] $n = 3$/condition; values in parentheses are the standard deviations.
[b] Turbidity was only measured for 37 °C.
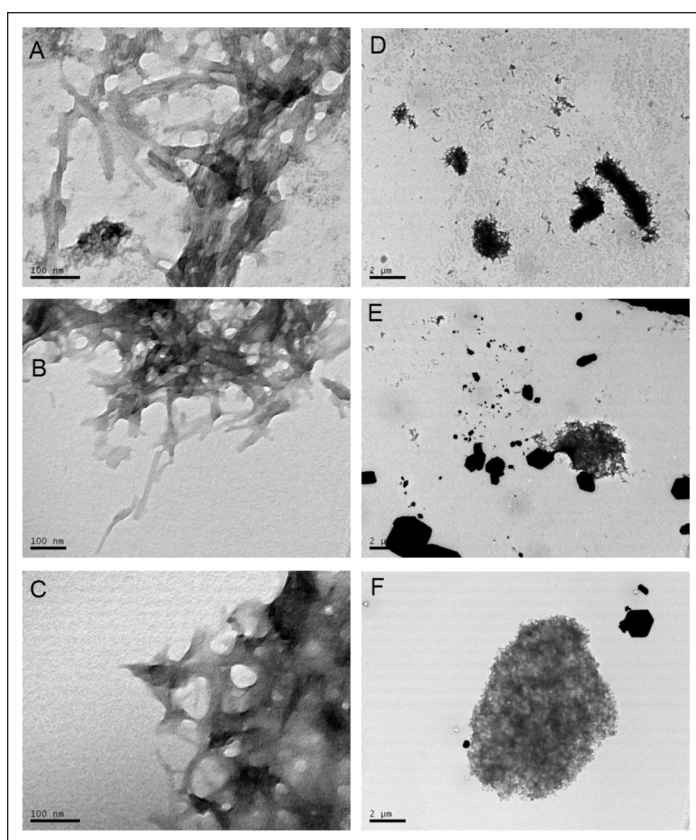
Transmission Electron Microscopy

Figure 4 shows TEM images of the fibrous insoluble insulin material formed at 45 °C. The short fibrils are layered in complex mats, making individual fibrils difficult to examine. This high density of the fibril mats may be related to the insulin concentration.[56] Higher magnifications (140,000–190,000x) reveal fibrils of up to 200 nm in length with diameters of 10–20 nm. The diameters are typical of insulin fibrils, but the short lengths are atypical. Human and bovine insulin fibrils are usually several micrometers long.[21,22,56,57] However, the longer heating and agitation times used in this study may have resulted in shorter fibrils due to fragmentation, similar to studies on other amyloidogenic proteins.[49,51]

Aspart and glulisine fibrils are better resolved at higher magnification. The striated ribbon-like morphologies of these fibrils suggest a lateral association of the individual protofilaments.[21] Although mature insulin fibrils often have a twisted appearance, striated ribbon-like structures have been reported.[21,57] In similar work, the amyloidogenic peptide $A\beta_{1-40}$ showed striated ribbon-like fibril morphology after agitation, while static intrinsic fibrillation conditions favored a twisted morphology.[58,59] The morphology of these fibrils may also be inherent to the amino acid sequence substitutions of insulin analogs, regardless of external conditions.

Lower magnifications show dense micrometer-scale clusters containing many individual fibrils, with analog-dependent size variation. Aspart and glulisine form clusters of less than 3 μm in diameter, while lispro forms larger clusters up to 8 μm. Although these clusters may form during drying on the TEM grid, they may also exist in suspension. Insulin fibrils readily associate, and suspended clusters of fibrils up to 100 μm in diameter have been detected by small-angle light scattering.[60] Both fibril formation and association may have implications for device compatibility and possible immunological outcomes.

Kinetic Analysis of Intrinsic Fibrillation in 96-Well Plate Format

The nucleation-dependent process of protein fibrillation is usually described by two parameters: lag time and growth rate.[49] These parameters reflect the efficiency of nucleation and polymerization processes, respectively. Changing conditions (reaction temperature, agitation, or protein primary structure) can affect either or both parameters. Periodic sampling of the incubated insulin solutions reveals discernable differences in intrinsic

Figure 4. Transmission electron microscopy images of fast-acting insulin fibrils formed at 45 °C after agitation of insulin solutions in PBS for 5 days: **(A, D)** aspart, **(B, E)** glulisine, and **(C, F)** lispro. Magnification is 140,000–190,000x for **(A–C)** (100 nm ruler) and 7200x for **(D–F)** (2 μm ruler).

fibrillation rates among the different insulin analogs (**Figure 2**) but prevents sensitive determination of kinetic parameters due to lower intermittent sampling frequency.

To compare insulin analog intrinsic fibrillation kinetics with greater accuracy, turbidity studies measuring optical density at 600 nm were carried out in a sealed 96-well plate in a temperature-controlled UV–Vis reader, with automatic turbidity measurement (optical density at 600 nm) every 400 s. The elevated temperature of 45 °C was chosen to speed the intrinsic fibrillation process and reduce replicate variability. Turbidity and fluorescent dyes have both been used previously for kinetic intrinsic fibrillation studies of proteins and peptides,[61–65] and automated 96-well plate assays have been carried out with the fluorescent dyes *in situ*.[61,64,66] Thioflavine T can delay insulin intrinsic fibrillation under certain conditions,[22] and we have demonstrated substantially longer intrinsic fibrillation lag times for aspart and glulisine, but not lispro, in the presence of ThT (data not shown). This differential effect of *in situ* ThT on insulin analog intrinsic fibrillation prevents colorimetric

kinetic analyses. However, the results from intermittent sampling studies shown in **Figure 3** and **Table 3** confirm turbidity as an effective marker of insulin intrinsic fibrillation, with sufficient resolution to observe differences between analogs. The initial studies discussed earlier demonstrated the efficacy of various methods for comparison of analog insulin intrinsic fibrillation rates. For this higher-resolution kinetic analysis, native human insulin was also included as a baseline control.

Figure 5 shows the average turbidity plots for the three fast-acting insulin analogs and human insulin. The higher sampling rate of the 96-well plate method gives better estimates of lag time prior to intrinsic fibrillation initiation and detects transitions occurring throughout the fibril growth phase. In agreement with the intermittent sampling results in **Figure 2**, aspart demonstrated a shorter lag time than glulisine or lispro. Control recombinant human insulin demonstrated a shorter lag time and faster fibril growth rate than any of the three fast-acting analogs. Human insulin also gave a higher overall turbidity signal, reflecting possible differences in particle number and particle size. The determined rate constants and lag times for human insulin were similar to those observed in previous insulin fibrillation studies,[17] although the exact experimental conditions varied.

Figure 6 examines the relationships between fibril growth rate, calculated during the region of fastest fibril propagation, and lag time.[17] Among proteins and peptides that form amyloid fibrils, longer lag times generally lead to slower growth rates.[66,67] The increased time lag and
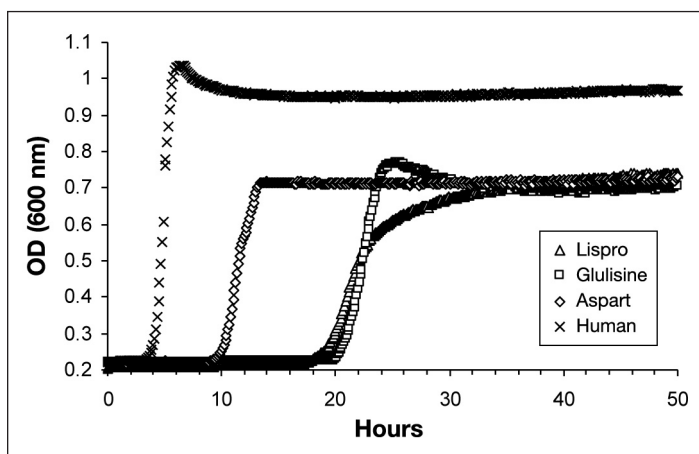
slower fibril propagation for analogs versus recombinant human insulin suggest greater monomer stability, slower fibril nucleus formation, and/or slower monomer recruitment into growing fibrils. A near-linear inverse correlation exists between the growth rate and lag time for human insulin, aspart, and lispro. Both analogs contain amino acid substitutions for the B28 proline of human insulin, which is a key residue in β-sheet interactions during dimerization, and may also inhibit the formation of β-sheet-rich fibrils.

The linear correlation does not extend to glulisine, which has a lag time close to lispro but a growth rate similar to aspart. An intramolecular salt bridge at the B29 glutamic acid position imparts greater stability to the glulisine monomer.[37] This may slow the partial monomer unfolding required for nucleus formation, resulting in a longer lag time. After intrinsic fibrillation initiation, the overall thermodynamic favorability of fibril growth may negate this monomer-stabilizing effect, leading to a faster growth rate.

The increased lag times and slower rates for the three analogs versus regular human insulin may appear contradictory considering the relative importance of reactive monomers in a nucleation-dependent polymerization model of the amyloid fibrillation process.[68] Work on insulin lispro fibrillation designed to mimic the low pH (3.0) conditions of insulin manufacturing processes, and with intentional addition of seeding nuclei, showed increased rates of insulin lispro fibril formation.[69] However, multiple alternative insulin fibrillation nucleation and
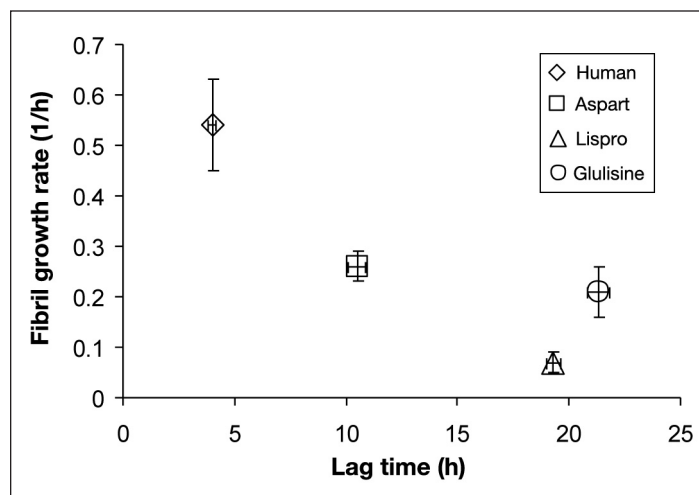

Figure 5. Intrinsic fibrillation kinetics of recombinant human insulin and three fast-acting insulin analogs monitored by turbidity (optical density at 600 nm). Plots are the averages of four or five replicates per analog. OD, optical density.

Figure 6. Intrinsic fibrillation lag times and fibril growth rates for recombinant human insulin and insulin analogs. Results are averages of four or five replicates per insulin type. Error bars are ± 1 standard deviation for both lag time (x error) and growth rate (y error).

propagation mechanisms have been proposed, and the variability of the fibrillation process with multiple factors (temperature, pH, ionic strength, insulin concentration, insulin structure, formulation additives) is well-known but insufficiently understood.[68] Since much of this historical work has been performed with regular insulin, additional effort is needed to examine the fibrillation process with the insulin analogs currently in common use.

Conclusions

This study is the first examination and comparison of the intrinsic amyloid fibril formation potential for fast-acting insulin analogs. This study examined the analogs after removal of the stabilizing excipients that are added to the commercial formulations, but at the lower temperatures, neutral pH, and insulin concentrations similar to what could be encountered with potential misuse (e.g., vehicle storage during summer months). Although all analogs appear more stable than human insulin, each is susceptible to fibril formation. The comparative lag times for fibril initiation, rates of fibril propagation, and fibril morphology also differ between the analogs. Marketed analog formulations also contain stabilizing excipients—the preservatives, *m*-cresol and phenol—in lispro and aspart to promote a more stable hexameric structure, while a polysorbate surfactant stabilizes the glulisine monomer. This study represents a "worst-case" scenario in which these stabilizing excipients are lost and insulin is subjected to harsh heating and agitation. These studies are not intended to provide a complete mechanistic understanding of insulin analog fibrillation or examination of the multiple potential critical parameters involved, but rather provide preliminary comparative data and methodology. Corollary work using enhanced analytical methods for detecting aggregation states and critical factors remains ongoing. This work underscores the need for proper storage and handling of insulin and insulin-containing devices. Similarly, as use of fast-acting insulin analogs grows and new delivery systems are developed, it is imperative to fully understand the mechanisms of insulin fibril formation using effective methods to test for and minimize this degradation during usage.

References:

1. Mahler HC, Friess W, Grauschopf U, Kiese S. Protein aggregation: pathways, induction factors and analysis. J Pharm Sci. 2009;98(9):2909–34.

2. Manning MC, Chou DK, Murphy BM, Payne RW, Katayama DS. Stability of protein pharmaceuticals: an update. Pharm Res. 2010;27(4):544–75.

3. Weiss WF 4th, Young TM, Roberts CJ. Principles, approaches, and challenges for predicting protein aggregation rates and shelf life. J Pharm Sci. 2009;98(4):1246–77.

4. Patel J, Kothari R, Tunga R, Ritter NM, Tunga BS. Stability considerations for biopharmaceuticals, part 1. BioProc Int. 2011;9:20–31.

5. Morozova-Roche L, Malisauskas M. A false paradise - mixed blessings in the protein universe: the amyloid as a new challenge in drug development. Curr Med Chem. 2007;14(11):1221–30.

6. Wang W. Protein aggregation and its inhibition in biopharmaceutics. Int J Pharm. 2005;289(1-2):1–30.

7. Maas C, Hermeling S, Bouma B, Jiskoot W, Gebbink MF. A role for protein misfolding in immunogenicity of biopharmaceuticals. J Biol Chem. 2007;282(4):2229–36.

8. Rosenberg AS. Effects of protein aggregates: an immunologic perspective. AAPS J. 2006;8(3):E501–7 .

9. Chiti F, Webster P, Taddei N, Clark A, Stefani M, Ramponi G, Dobson CM. Designing conditions for *in vitro* formation of amyloid protofilaments and fibrils. Proc Natl Acad Sci USA.1999;96(7):3590–4.

10. Taylor JP, Hardy J, Fischbeck KH. Toxic proteins in neuro-degenerative disease. Science. 2002;296(5575):1991–5.

11. Ross CA, Poirier MA. Protein aggregation and neurodegenerative disease. Nat Med. 2004;10 Suppl:S10–7.

12. Rochet JC, Lansbury PT Jr. Amyloid fibrillogenesis: themes and variations. Curr Opin Struct Biol. 2000;10(1):60–8.

13. Nelson R, Sawaya MR, Balbirnie M, Madsen AØ, Riekel C, Grothe R, Eisenberg D. Structure of the cross-beta spine of amyloid-like fibrils. Nature. 2005;435(7043):773–8.

14. Petkova AT, Ishii Y, Balbach JJ, Antzutkin ON, Leapman RD, Delaglio F, Tycko R. A structural model for Alzheimer's beta-amyloid fibrils based on experimental constraints from solid state NMR. Proc Natl Acad Sci USA. 2002;99(26):16742–7.

15. Tycko R. Progress towards a molecular-level structural understanding of amyloid fibrils. Curr Opin Struct Biol. 2004;14(1):96–103.

16. Brange J, Andersen L, Laursen ED, Meyn G, Rasmussen E. Toward understanding insulin fibrillation. J Pharm Sci. 1997;86(5):517–25.

17. Nielsen L, Khurana R, Coats A, Frokjaer S, Brange J, Vyas S, Uversky VN, Fink AL. Effect of environmental factors on the kinetics of insulin fibril formation: elucidation of the molecular mechanism. Biochemistry. 2001;40(20):6036–46.

18. Sluzky V, Tamada JA, Klibanov AM, Langer R. Kinetics of insulin aggregation in aqueous solutions upon agitation in the presence of hydrophobic surfaces. Proc Natl Acad Sci USA. 1991;88(21):9377–81.

19. Sluzky V, Klibanov AM, Langer R. Mechanism of insulin aggregation and stabilization in agitated aqueous solutions. Biotechnol Bioeng. 1992;40(8):895–903.

20. Ahmad A, Millett IS, Doniach S, Uversky VN, Fink AL. Partially folded intermediates in insulin fibrillation. Biochemistry. 2003;42(39):11404–16.

21. Jiménez JL, Nettleton EJ, Bouchard M, Robinson CV, Dobson CM, Saibil HR. The protofilament structure of insulin amyloid fibrils. Proc Natl Acad Sci USA. 2002;99(14):9196–201.

22. Manno M, Craparo EF, Podestà A, Bulone D, Carrotta R, Martorana V, Tiana G, San Biagio PL. Kinetics of different processes in human insulin amyloid formation. J Mol Biol. 2007;366(1):258–74.

23. Ahmad A, Uversky VN, Hong D, Fink AL. Early events in the fibrillation of monomeric insulin. J Biol Chem. 2005;280(52):42669–75.

24. Ivanova MI, Sievers SA, Sawaya MR, Wall JS, Eisenberg D. Molecular basis for insulin fibril assembly. Proc Natl Acad Sci USA. 2009;106(45):18990–5.

25. Groenning M, Frokjaer S, Vestergaard B. Formation mechanism of insulin fibrils and structural aspects of the insulin fibrillation process. Curr Protein Pept Sci. 2009;10(5):509–28.

26. Guilhem I, Leguerrier AM, Lecordier F, Poirier JY, Maugendre D. Technical risks with subcutaneous insulin infusion. Diabetes Metab. 2006;32(3):279–84.

27. Pryce R. Diabetic ketoacidosis caused by exposure of insulin pump to heat and sunlight. BMJ. 2009;338:a2218.

28. Rahuel-Clermont S, French CA, Kaarsholm NC, Dunn MF, Chou CI. Mechanisms of stabilization of the insulin hexamer through allosteric ligand interactions. Biochemistry. 1997;36(19):5837–45.

29. Whittingham JL, Edwards DJ, Antson AA, Clarkson JM, Dodson GG. Interactions of phenol and m-cresol in the insulin hexamer, and their effect on the association properties of B28 pro --> Asp insulin analogues. Biochemistry. 1998;37(33):11516–23.

30. Derewenda U, Derewenda Z, Dodson EJ, Dodson GG, Reynolds CD, Smith GD, Sparks C, Swenson D. Phenol stabilizes more helix in a new symmetrical zinc insulin hexamer. Nature. 1989;338(6216):594–6.

31. Bakaysa DL, Radziuk J, Havel HA, Brader ML, Li S, Dodd SW, Beals JM, Pekar AH, Brems DN. Physicochemical basis for the rapid time-action of LysB28ProB29-insulin: Dissociation of a protein-ligand complex. Protein Sci. 1996;5(12):2521–31.

32. Ciszak E, Beals JM, Frank BH, Baker JC, Carter ND, Smith GD. Role of C-terminal B-chain residues in insulin assembly: the structure of hexameric LysB28ProB29-human insulin. Structure. 1995;3(6):615–22.

33. Richards JP, Stickelmeyer MP, Flora DB, Chance RE, Frank BH, DeFelippis MR. Self-association properties of monomeric insulin analogs under formulation conditions. Pharm Res. 1998;15(9):1434–41.

34. Raskin P, Guthrie RA, Leiter L, Riis A, Jovanovic L. Use of insulin aspart, a fast-acting insulin analog, as the mealtime insulin in the management of patients with type 1 diabetes. Diabetes Care. 2000;23(5):583–8.

35. Brange J, Vølund A. Insulin analogs with improved pharmaco-kinetic profiles. Adv Drug Deliv Rev. 1999;35(2-3):307–35.

36. Hirsch IB. Insulin analogues. N Engl J Med. 2005;352(2):174–83.

37. Becker RH. Insulin glulisine complementing basal insulins: a review of structure and activity. Diabetes Technol Ther. 2007;9(1):109–21.

38. Holleman F, Hoekstra JB. Insulin lispro. N Engl J Med. 1997;337(3):176–83.

39. Kerwin BA. Polysorbates 20 and 80 used in the formulation of protein biotherapeutics: structure and degradation pathways. J Pharm Sci. 2008;97(8):2924–35.

40. Harrison DM, Garratt CJ. The accurate measurement of insulin molarity. Biochem J. 1969;113(4):733–4.

41. Krüger P, Gilge G, Cabuk Y, Wollmer A. Cooperativity and intermediate states in the T----R-structural transformation of insulin. Biol Chem Hoppe Seyler. 1990;371(8):669–73.

42. Teska B, Alarcon J, Pettis RJ, Randolph T, Carpenter J. Effect of phenol and m-cresol depletion on analog insulin conformational stability. AAPS J. 2011;12:S1. http://www.aapsj.org/abstracts/NBC_2011/T2077.pdf. Accessed January 12, 2012.

43. Kodali R, Wetzel R. Polymorphism in the intermediates and products of amyloid assembly. Curr Opin Struct Biol. 2007;17(1):48–57.

44. LeVine H 3rd. Quantification of beta-sheet amyloid fibril structures with thioflavin T. Methods in Enzymol. 1999;309:274–84.

45. Groenning M, Norrman M, Flink JM, van de Weert M, Bukrinsky JT, Schluckebier G, Frokjaer S. Binding mode of Thioflavin T in insulin amyloid fibrils. J Struct Biol. 2007;159(3):483–97.

46. Meinhardt J, Sachse C, Hortschansky P, Grigorieff N, Fändrich M. Abeta(1-40) fibril polymorphism implies diverse interaction patterns in amyloid fibrils. J Mol Biol. 2009;386(3):869–77.

47. Nelson R, Sawaya MR, Balbirnie M, Madsen AØ, Riekel C, Grothe R, Eisenberg D. Structure of the cross-beta spine of amyloid-like fibrils. Nature. 2005;435(7043):773–8.

48. Pedersen JS, Dikov D, Flink JL, Hjuler HA, Christiansen G, Otzen DE. The changing face of glucagon fibrillation: structural polymorphism and conformational imprinting. J Mol Biol. 2006;355(3):501–23.

49. Hortschansky P, Schroeckh V, Christopeit T, Zandomeneghi G, Fändrich M. The aggregation kinetics of Alzheimer's beta-amyloid peptide is controlled by stochastic nucleation. Protein Sci. 2005;14(7):1753–9.

50. Xue WF, Homans SW, Radford SE. Systematic analysis of nucleation-dependent polymerization reveals new insights into the mechanism of amyloid self-assembly. Proc Natl Acad Sci USA. 2008;105(26):8926–31.

51. Uversky VN, Li J, Fink AL. Evidence for a partially folded intermediate in alpha-synuclein fibril formation. J Biol Chem. 2001;276(14):10737–44.

52. Kusumoto Y, Lomakin A, Teplow DB, Benedek GB. Temperature dependence of amyloid beta-protein fibrillization. Proc Natl Acad Sci USA. 1998;95(21):12277–82.

53. Chiti F, Stefani M, Taddei N, Ramponi G, Dobson CM. Rationalization of the effects of mutations on peptide and protein aggregation rates. Nature. 2003;424(6950):805–8.

54. Hammarström P, Jiang X, Hurshman AR, Powers ET, Kelly JW. Sequence-dependent denaturation energetics: a major determinant in amyloid disease diversity. Proc Natl Acad Sci USA. 2002;99 Suppl 4:16427–32.

55. López de la Paz M, Serrano L. Sequence determinants of amyloid fibril formation. Proc Natl Acad Sci. 2004;101(1):87–92.

56. Andersen CB, Otzen D, Christiansen G, Rischel C. Glucagon amyloid-like fibril morphology is selected via morphology-dependent growth inhibition. Biochemistry. 2007;46(24):7314–24.

57. Bouchard M, Zurdo J, Nettleton EJ, Dobson CM, Robinson CV. Formation of insulin amyloid fibrils followed by FTIR simultaneously with CD and electron microscopy. Protein Sci. 2000;9(10):1960–7.

58. Paravastu AK, Leapman RD, Yau WM, Tycko R. Molecular structural basis for polymorphism in Alzheimer's beta-amyloid fibrils. Proc Natl Acad Sci USA. 2008;105(47):18349–54.

59. Petkova AT, Leapman RD, Guo Z, Yau WM, Mattson MP, Tycko R. Self-propagating, molecular-level polymorphism in Alzheimer's beta-amyloid fibrils. Science. 2005;307(5707):262–5.

60. Manno M, Craparo EF, Martorana V, Bulone D, San Biagio PL. Kinetics of insulin aggregation: disentanglement of amyloid fibrillation from large-size cluster formation. Biophys J. 2006;90(12):4585–91.

61. Zheng J, Liu C, Sawaya MR, Vadla B, Khan S, Woods RJ, Eisenberg D, Goux WJ, Nowick JS. Macrocyclic β-sheet peptides that inhibit the aggregation of a tau-protein-derived hexapeptide. J Am Chem Soc. 2011;133(9):3144–57.

62. Giehm L, Otzen DE. Strategies to increase the reproducibility of protein fibrillization in plate reader assays. Anal Biochem. 2010;400(2):270–81.

63. Evans KC, Berger EP, Cho CG, Weisgraber KH, Lansbury PT Jr. Apolipoprotein E is a kinetic but not a thermodynamic inhibitor of amyloid formation: Implications for the pathogenesis and treatment of Alzheimer disease. Proc Natl Acad Sci USA. 1995;92(3):763–7.

64. Kim YS, Randolph TW, Stevens FJ, Carpenter JF. Kinetics and energetics of assembly, nucleation, and growth of aggregates and fibrils for an amyloidogenic protein. Insights into transition states from pressure, temperature, and co-solute studies. J Biol Chem. 2002;277(30):27240–6.

65. Andersen CB, Otzen D, Christiansen G, Rischel C. Glucagon amyloid-like fibril morphology is selected via morphology-dependent growth inhibition. Biochemistry. 2007;46(24):7314–24.

66. Brange J. The new era of biotech insulin analogues. Diabetologia. 1997;40 Suppl 2:S48–53.

67. Fändrich M 2007. Absolute correlation between lag time and growth rate in the spontaneous formation of several amyloid-like aggregates and fibrils. J Mol Biol. 2007;365(5):1266–70.

68. Groenning M, Frokjaer S, Vestergaard B. Formation mechanism of insulin fibrils and structural aspects of the insulin fibrillation process. Curr Protein Pept Sci. 2009;10(5):509–28.

69. Ludwig DB, Webb JN, Fernández C, Carpenter JF, Randolph TW. Quaternary conformational stability: The effect of reversible self-association on the fibrillation of two insulin analogs. Biotechnol Bioeng. 2011. Epub ahead of print.